Macromolecules **2001,** *34,* 3503−3506

Fast and Easy Flow-Alignment Technique of Lyotropic Liquid-Crystalline Hexagonal Phases of Block Copolymers and Surfactants

M. Impéror-Clerc,*,† I. W. Hamley,‡ and P. Davidson†

Laboratoire de Physique des Solides (UMR 8502 CNRS),
Bât. 510, Université Paris Sud, 91405 Orsay Cedex, France,
and School of Chemistry, University of Leeds,
Leeds LS2 9JT, United Kingdom

Received December 27, 2000

Introduction

Mesophases with hexagonal symmetry are widespread in the field of soft matter physics. They are observed for compounds as diverse as stiff linear polymers, block copolymers, amphiphilic molecules in a solvent, and disklike molecules.[1−4] In contrast with the nematic and lamellar structures, hexagonal mesophases, in most cases, are very viscous and do not align in a magnetic field. Structural studies are then usually performed on powder samples, which results in a loss of very useful information. In the past few years, several attempts have been made to produce single domains of hexagonal phase by various shear processes, but these techniques involve specialist equipment and are not simple to use.[5−11] In a recent article, we described how single domains of a lyotropic hexagonal mesophase can easily be produced merely by sucking material into optical flat glass capillaries with a vacuum pump.[12] This new technique was illustrated with the hexagonal phase found in the ternary phase diagram of sodium dodecyl sulfate (SDS) ionic surfactant, pentanol, and water. The purpose of the present note is to demonstrate by optical microscopy and X-ray scattering that our alignment procedure can be applied to the lyotropic hexagonal mesophases of block copolymers and of nonionic surfactants and that it is therefore quite general. Moreover, the aligned samples produced with this method undergo on cooling a thermomechanical instability, already described by Oswald et al. (ref 13), by which the columns show undulations or zigzag conformations.[12,13] This instability is due to the contraction of the 2-dimensional (2D) lattice in the vial and easily gives information on the mechanical constants of the mesophase.

Experimental Section

The $C_{12}E_6$ nonionic surfactant (*n*-dodecyl hexaethylene glycol ether) was purchased from Nikko Chemicals and used as received. The $E_{18}B_{10}$ diblock copolymer ((ethylene oxide)$_{18}$−(butylene oxide)$_{10}$) was kindly provided by Dow Chemical Co. Homogeneous mixtures of 49.6 wt % $C_{12}EO_6$ and 50.4 wt % water were prepared by weighing in test tubes the appropriate amounts of components and mixing them carefully. Mixtures of 35.0 wt % $E_{18}B_{10}$ and 65.0 wt % water were prepared in the same way.

Aligned samples of the hexagonal phases of both mixtures were easily obtained in flat optical glass capillaries (Vitro Com Inc., Mountain Lakes, NJ) of thicknesses 50 or 100 μm by sucking material into the capillaries with a vacuum pump at room temperature, as described in more detail in ref 12.

The samples were then observed in polarized light with a Leitz Orthoplan microscope, and their textures were recorded with a CCD video camera. The microscope was also equipped with a homemade computer-driven heating stage.

X-ray scattering experiments (Figures 3 and 4) were performed at the H10 experimental station of the LURE synchrotron radiation facility in Orsay, France.[15] A wavelength of $\lambda = 0.155$ nm was selected by the two-crystal monochromator. Harmonic rejection was obtained by reflection of the X-ray beam on two mirrors covered with rhodium. The beam size on the sample was 0.5×2 mm^2. The sample was set at the center of a Huber diffractometer equipped with a crystal analyzer (Ge 111). The scattered X-rays were detected either with imaging plates or with a Bicron point detector after reflection on the crystal analyzer. For temperature control, we used a homemade oven and a computer-driven temperature controller.

Additional X-ray scattering experiments (Figure 5) were performed at the D2AM experimental station of the ESRF synchrotron radiation facility in Grenoble, France.[16] A similar experimental setup was used, except that the detection was made using a CCD camera detector (Princeton Instruments, NJ).

Results and Discussion

Figure 1a−d shows the optical textures of the flow-aligned samples of hexagonal phase of $C_{12}E_6$ and $E_{18}B_{10}$, observed in polarized light microscopy. The samples appear dark when their main axis is parallel to the polarizer−analyzer axes and bright when they lie at 45° with respect to these axes. Therefore, the flow-aligned samples are highly oriented all along the capillary axis, as will be further demonstrated by X-ray scattering below. Moreover, these samples become striated on cooling which is the optical signature of a thermomechanical instability (Figure 1e,f) in which the columns undergo a zigzag distortion.[12,13] In Figure 2, we show the dependence of the undulation wavelength and tilt amplitude with temperature for the compound $E_{18}B_{10}$. (These plots can be found in ref 13 for $C_{12}E_6$.) The undulation wavelength Λ is directly related to the elastic properties of the mesophase.[13] It is therefore interesting to note here that the value of Λ measured for $E_{18}B_{10}$ ($\Lambda \approx 6.5$ μm) is very similar to those of $C_{12}E_6$ and SDS ($\Lambda \approx 5$ μm in both cases), even though these molecules are of very different chemical natures.

X-ray scattering experiments (Figure 3) allow us to better characterize the alignment degree of the samples and the nature of the instability.[12,13] The values of the hexagonal lattice parameter at 25 °C are $a = 5.85$ nm for $C_{12}E_6$ and $a = 9.1$ nm for $E_{18}B_{10}$. The electron density contrast appears to be much weaker for $E_{18}B_{10}$ than for $C_{12}E_6$, because the diffraction peaks recorded with $E_{18}B_{10}$ have a much lower intensity.[14] The degree of alignment can be assessed by measuring the mosaic spread of the (10) reflection of the 2-dimensional hexagonal lattice. As expected, for both $C_{12}E_6$ and $E_{18}B_{10}$ samples, we find that the C_6 axis is oriented along the capillary main axis and that a family of (10) dense planes lies parallel to the capillary flat walls. Azimuthal “ϕ-scans” (Figure 4a,b) yielded ϕ-mosaic values of 0.1° and 3° for $C_{12}E_6$ and $E_{18}B_{10}$, respectively. Such values compare very well with other values reported in the literature. $C_{12}E_6$ samples systematically showed better

---

† Université Paris Sud.
‡ University of Leeds.
* Author for correspondence.

10.1021/ma0021951 CCC: $20.00

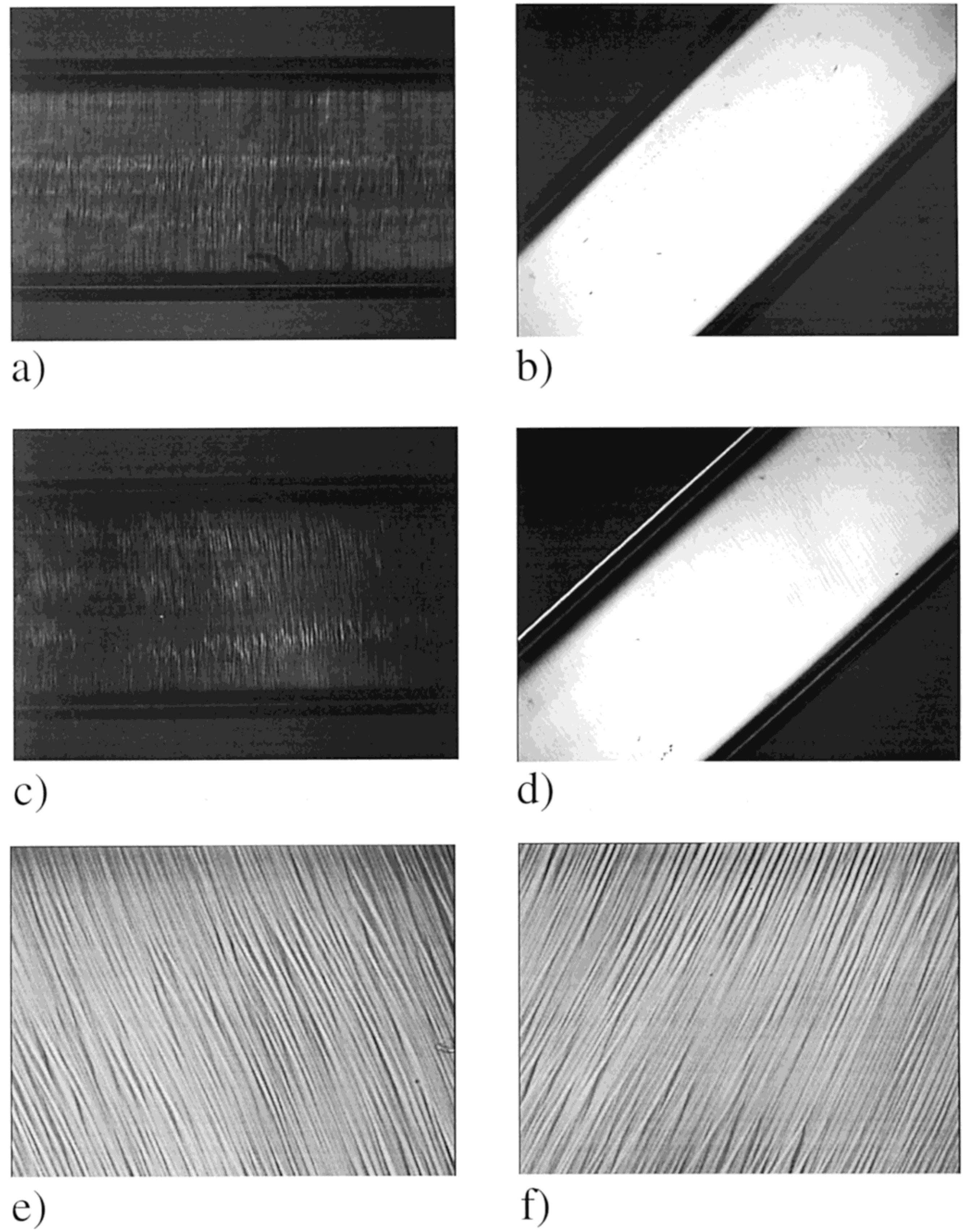

Figure 1. Photographs between crossed polarizers of rectangular glass capillaries (0.1 mm thick and 1 mm wide) at room temperature. α is the angle between the polarizer and the glass capillary axis. (a) $C_{12}E_6$, α = 0°; (b) $C_{12}E_6$, α = 45°; (c) $E_{18}B_{10}$, α = 0°; (d) $E_{18}B_{10}$, α = 45°; (e) $E_{18}B_{10}$, α = 15°, details of the zigzag texture; (f) $E_{18}B_{10}$, α = −15°, details of the zigzag texture.

alignment than $E_{18}B_{10}$ ones, possibly due to different viscoelastic properties and possibly also due to greater polydispersity of the latter. The mosaic spread in the other direction was measured by performing “χ-scans”, yielding values of 3° and 5° for $C_{12}E_6$ and $E_{18}B_{10}$, respectively.

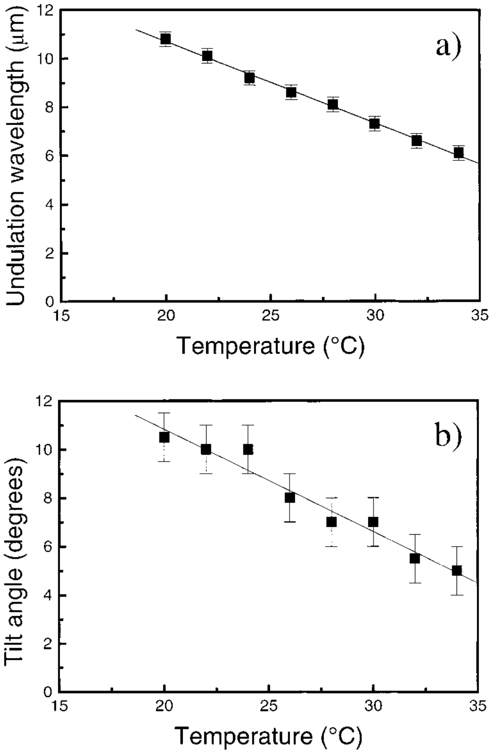

Figure 2. (a) Wavelength Λ of the zigzags vs temperature. (b) Zigzag angle θ vs temperature measured by the optical method developed in ref 13.

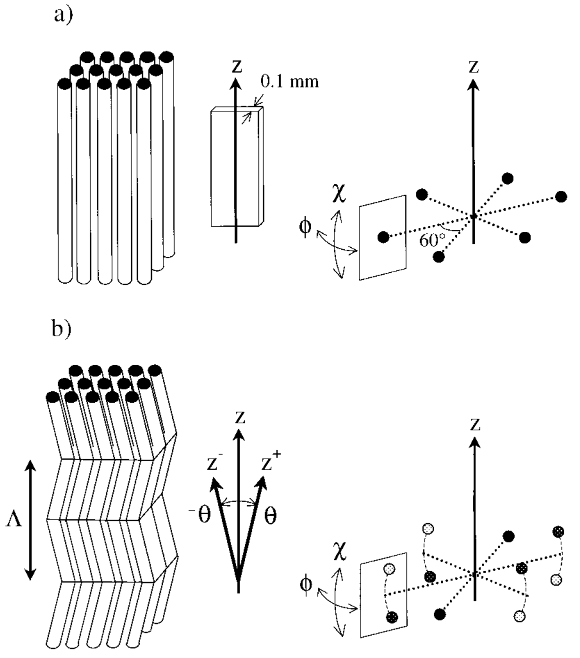

Figure 3. (a) Diffraction by a single domain of hexagonal phase. The Z-axis is along the columns. Six (10) Bragg reflections are observed in the perpendicular plane. The ϕ angle is the rotation angle around the Z-axis. The χ angle is the rotation angle inside the diffraction plane for a (10) Bragg peak. (b) Diffraction by a "zigzag" domain. Blocks of columns are periodically (spatial wavelength Λ) tilted in a plane by the angles θ and $-\theta$. The superposition of the diffraction by these two types of blocks gives rise to the splitting of four (10) Bragg spots. The two other (10) Bragg spots which are along the direction perpendicular to the zigzag plane are unchanged.

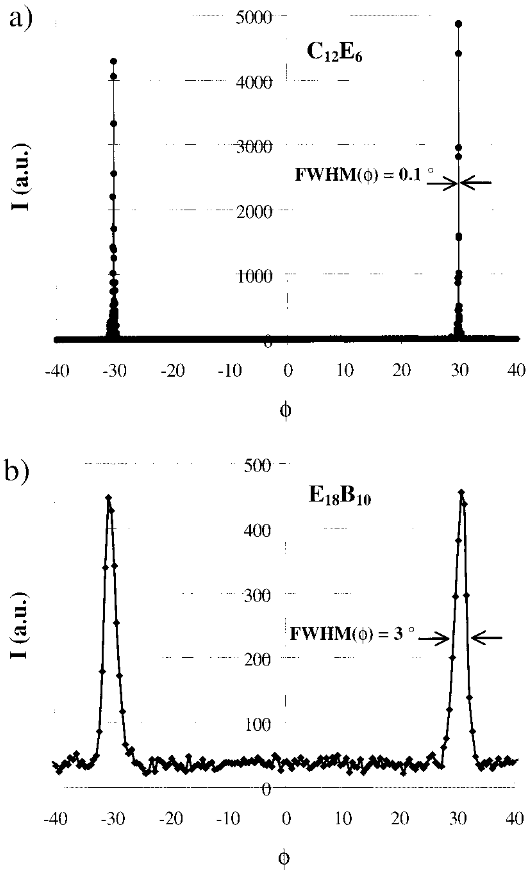

Figure 4. (a) ϕ-scan of a $C_{12}E_6$ aligned sample. (b) ϕ-scan of a $E_{18}B_{10}$ aligned sample.

The χ-mosaic is actually affected by the existence of the thermomechanical instability. Indeed, in contrast to SDS which has a negative dilation coefficient, we observed that both $C_{12}E_6$ and $E_{18}B_{10}$ have positive dilation coefficients ($\alpha = (1/a)(da/dT) = 3.2 \times 10^{-4}$ K^{-1} and $\alpha = 8.5 \times 10^{-4}$ K^{-1}, respectively) so that the instability appears on cooling.[12,13,17] The X-ray scattering signature of the instability lies in the splitting of four of the (10) reflections of the 2D hexagonal lattice. This splitting is due to the appearance of "zig" and "zag" domains which give rise to separate reflections (Figure 3 and Figure 5a,b). The splitting angle increases on cooling, indicating an increase in modulation amplitude as already inferred from optical microscopy. There again, both $C_{12}E_6$ and $E_{18}B_{10}$ samples show tilt angles that are similar to those of SDS ones. This splitting vanishes when the samples are heated again, which proves that the instability is reversible.

Conclusion

In this note, we have shown that sucking material in flat glass capillaries is a general, simple, fast, and cheap method to produce aligned samples of lyotropic hexagonal mesophases. The mosaic spreads of our samples measured by X-ray scattering compare very favorably with those of samples produced by other much more complex and time-consuming alignment techniques. The study of the thermomechanical instability of these aligned samples led us to conclude that the hexagonal mesophases of SDS, $C_{12}E_6$, and $E_{18}B_{10}$ have very similar mechanical properties despite their quite different chemical natures. The simple "capillary flow" technique described here may also find applications when molecular orientation is required such as in optical and spectroscopic investigations.

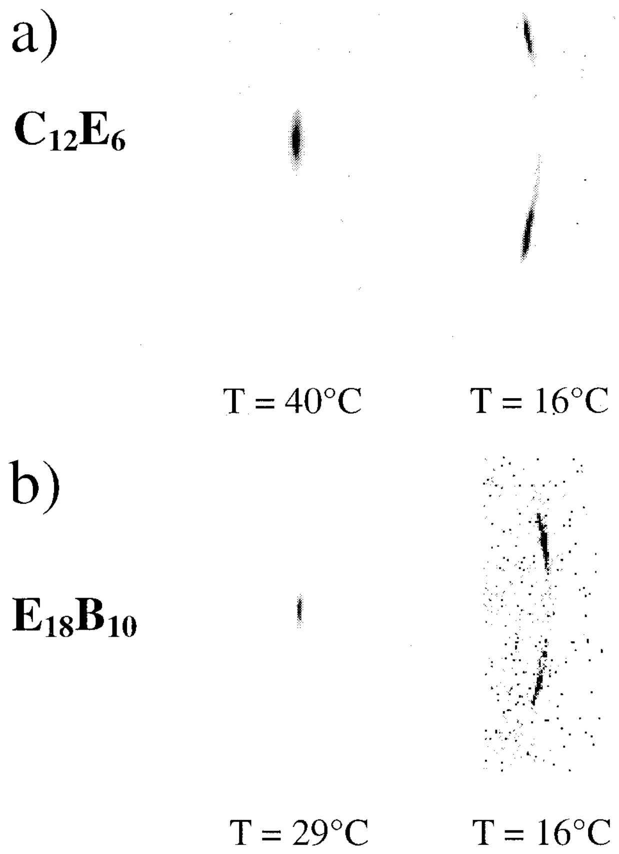

Figure 5. (a) Splitting of a (10) Bragg peak of a $C_{12}E_6$ sample on cooling a single domain from 40 to 16 °C at 1 °C /min. (b) Splitting of a (10) Bragg peak of a $E_{18}B_{10}$ sample on cooling a single domain from 29 to 16 °C at 1.5 °C /min.

Acknowledgment. We express our thanks to J. F. Bérar (ESRF), M. Gailhanou (LURE), and O. Pelletier for help during the X-ray scattering experiments and to V. Klein for building the heating stage electronics.

References and Notes

(1) Ungar, G. *Polymer* **1993**, *34*, 2050.
(2) Hamley, I. W. *The Physics of Block Copolymers*; Oxford University Press: New York, 1998.
(3) Hendrikx, Y.; Levelut, A. M. *Mol. Cryst. Liq. Cryst.* **1988**, *165*, 233.
(4) Levelut, A. M. *J. Chim. Phys.* **1983**, *80*, 409.
(5) Safinya, C. R.; Liang, K. S.; Varady, W. A.; Clark, N. A.; Andersson, G. *Phys. Rev. Lett.* **1984**, *53*, 1172.
(6) Fontes, E.; Heiney, P. A.; Ohba, M.; Haseltine, J. N.; Smith, A. B. *Phys. Rev. A* **1988**, *37*, 1329.
(7) Koltover, I.; Idziak, S. H. J.; Davidson, P.; Li, Y.; Safinya, C. R.; Ruths, M.; Steinberg, S.; Israelachvili, J. N. *J. Phys. II* **1996**, *6*, 893.
(8) Hamley, I. W.; Koppi, K. A.; Rosedale, J. H.; Bates, F. S.; Almdal, K.; Mortensen, K. *Macromolecules* **1993**, *26*, 5959.
(9) Bates, F. S.; Koppi, K. A.; Tirrell, M.; Almdal, K.; Mortensen, K. *Macromolecules* **1994**, *27*, 5934.
(10) Schmidt, G.; Müller, S.; Lindner, P.; Schmidt, C.; Richtering, W. *J. Phys. Chem B* **1998**, *102*, 507.
(11) Ramos, L.; Molino, F.; Porte, G. *Langmuir* **2000**, *16*, 5846.
(12) Impéror-Clerc, M.; Davidson, P. *Eur. Phys. J. B* **1999**, *9*, 93.
(13) Oswald, P.; Géminard, J. C.; Lejcek, L.; Sallen, L. *J. Phys. II* **1996**, *6*, 281.
(14) Simple estimations of the electronic densities give 334 e^{-}/nm^3 for water, 276 e^{-}/nm^3 for a C_{12} chain, 366 e^{-}/nm^3 for a E (ethylene oxide) corona, and 335 e^{-}/nm^3 for a B (butylene oxide) core. For $C_{12}E_6$, the contrast arises mainly from the difference between the C_{12} chains and water. For $E_{18}B_{10}$, the contrast only arises from the E corona and is then very weak.
(15) Gailhanou, M.; Dubuisson, J. M.; Ribbens, M.; Roussier, L.; Bétaille, D.; Créoff, C.; Lemonnier, M.; Denoyer, J.; Jucha, A.; Lena, A.; Idir, M.; Bessière, M.; Thiaudière, D.; Hennet, L.; Landron, C.; Coutures, J. P. *Nucl. Instrum. Methods, Sect. A,* in press.
(16) (a) Simon, J. P.; Geissler, E.; Hecht, A. M.; Bley, F.; Livet, F.; Roth, M.; Ferrer, J. L.; Fanchon, E.; Cohen-Addad, C.; Thierry, J. C. *Rev. Sci. Instrum.* **1992**, *63*, 1051. (b) Bérar, J. F.; Simon, J. P.; Ferrer, J. L.; Dallé, D. *Mater. Sci. Forum* **1996**, *228−231*, 223.
(17) Constantin, D.; Oswald, P.; Impéror-Clerc, M.; Davidson, P.; Sotta, P. *J. Phys. Chem. B* **2001**, *105*, 668.

MA0021951